Electronic Supplementary Material (ESI) for Analyst.

Fabrication of a Sustainable Superhydrophobic Surface of Ag-NPs @SA on Copper Alloy for corrosion resistance, photocatalysis, and Simulated distribution of Ag atoms

Noor Hassan[a*], Zeeshan Ajmal[a], Sun Liang heng[b*], Khaled Fahmi Fawy[c], Sajid Mahmood[d], Fazila Mushtaq[e], Munirah D. Albaqami[f], Saikh Mohammad[g], Raqiqa Tur Rasool[h], Ghulam Abbas Ashraf[i*].

[a] College of Chemistry and Material Sciences, Zhejiang Normal University, Jinhua, 321004, Zhejiang, China.

[b] Rail Transit College, Chengdu lndustry and Trade College, Chengdu, 611730, China.

[c] Department of Chemistry, Faculty of Science, King Khalid University, P.O. Box 9004, Abha 61413, Saudi Arabia.

[d] Green Chemicals & Energy Process Development Laboratory, China Beacons Institute, University of Nottingham Ningbo, Ningbo 315040, China

[e] Institute of Chemical Sciences, Bahauddin Zakariya University, Multan, Pakistan.

[f, g] Department of Chemistry, College of Science, King Saud University, Riyadh 11451, Saudi Arabia

[h] Department of Physics, Zhejiang Normal University, Jinhua, Zhejiang, 321004, China.

[i] Key Laboratory of Integrated Regulation and Resources Development on Shallow Lake of Ministry of Education, College of Environment, Hohai University, Nanjing 210098, China.

Corresponding author: raviannoor80@hotmail.com (N.Hassan), 13086601167@163.com (S. L. Heng), ga_phy@yahoo.com (G. A. Ashraf).

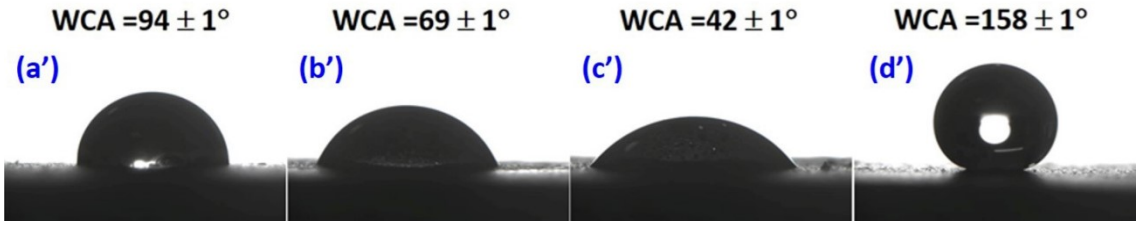

Fig. S1. Digital images of WCAs on copper alloy substrates: WCA on the bare copper alloy (a′), WCA of the Cu-sheet after chemical etching (b′), WCA of the copper substrate after immersion in silver nitrate solution (c′), and water CA of copper alloy plate after thermal annealing treatment (d′).

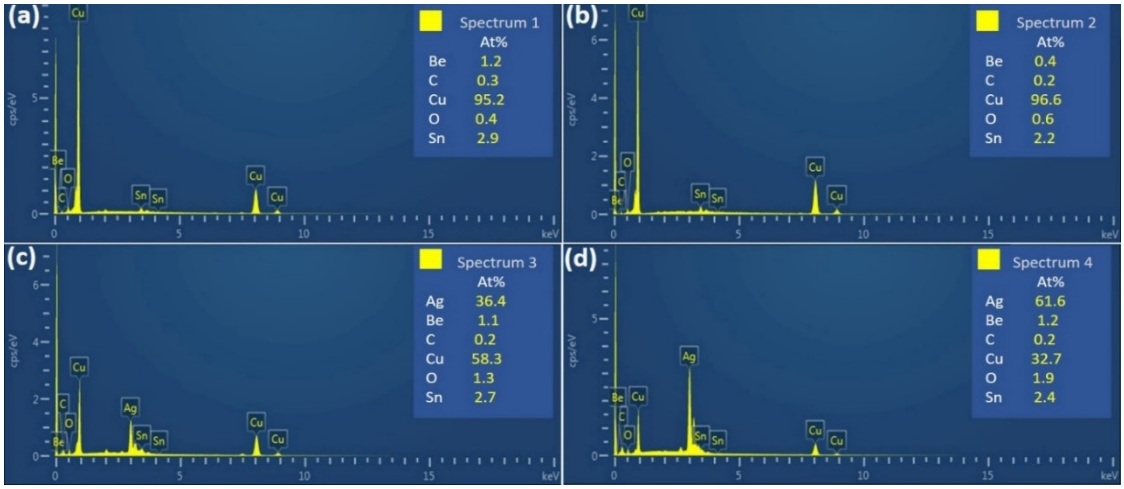

Fig. S2. EDS investigation of the samples: (a) non-coated copper alloy, (b) surface of the etched copper alloy (c) surface of the copper alloy after immersion in the aqueous solution of $AgNO_3$, and (d) the image of copper alloy on which Ag-NPs were coated and then finally annealed.

1. Experimental Parameters Affecting the Wettability

1.1. The concentration of the Coating solution

It is a key step to find out the factors that affect the surface wettability of the copper alloy. It was focused on the immersion concentration and immersion time which affects wettability (Wang et al., 2015). The proper immersion concentration of the concerned solutions and immersion time are important, which provide hydrophobicity on the complete surface. Fig. S3 demonstrates the variation in static water contact angles towards the surface of copper alloy through the immersion concentrations and immersion time, separately. The sheets of copper alloy were chemically etched with 2M HNO_3 solution for 7 minutes. Thereafter these etched substrates were dipped in the aqueous solution of silver nitrate of 0.0035, 0.045, 0.0055, 0.0065, 0.0075, and 0.0085 mmol with the constant immersion time of 20 minutes, and thermal annealing treatment is performed in the electric oven at constant temperature scale of 155 °C for 1 hour.

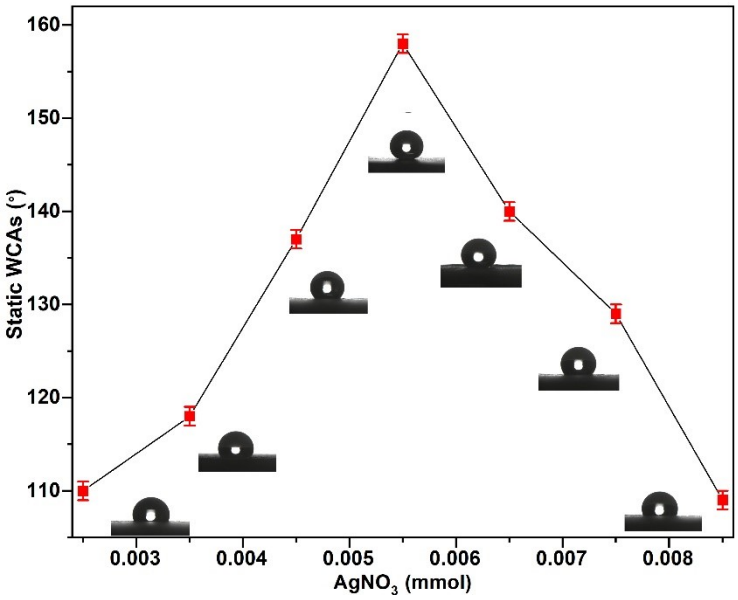

Fig. S3. WCAs of the as-prepared surfaces for 7 min in 2 mol·L^{-1} HNO_3 solution while immersed in 5.5 mmol·L^{-1} $AgNO_3$ solution for 20 min, followed by annealing at 155 ºC for 1 h along with different concentrations of $AgNO_3$ solutions.

The most excellent static water CA of 158±1° was observed, which showed up in the aqueous $AgNO_3$ solution of 5.5 mmol L^{-1} as well as adding the CAs of static water at different focuses were similarly greater than 150°. Consequently, the concentration impact of the aqueous solution of $AgNO_3$ does not make much difference, it may be valuable for the construction of larger surface areas, and, after that, it may advance industrially.

1.2. Immersion Time

The effect of immersion time on the surface wettability was also investigated at the different immersing time intervals for the copper substrate (Song et al., 2012). The samples were immersed in the 5.5 mmol silver nitrate solutions that chemically reacted for 5, 10, 15, 20, 25, 30, and 35 minutes under similar conditions that appeared in Fig. S4. The WCAs obtained are approximately 141±1°, but the most significant static water CA of 158±1° was obtained by 20 min immersing, as represented in Fig. 3(d-f), which demonstrated superhydrophobicity.

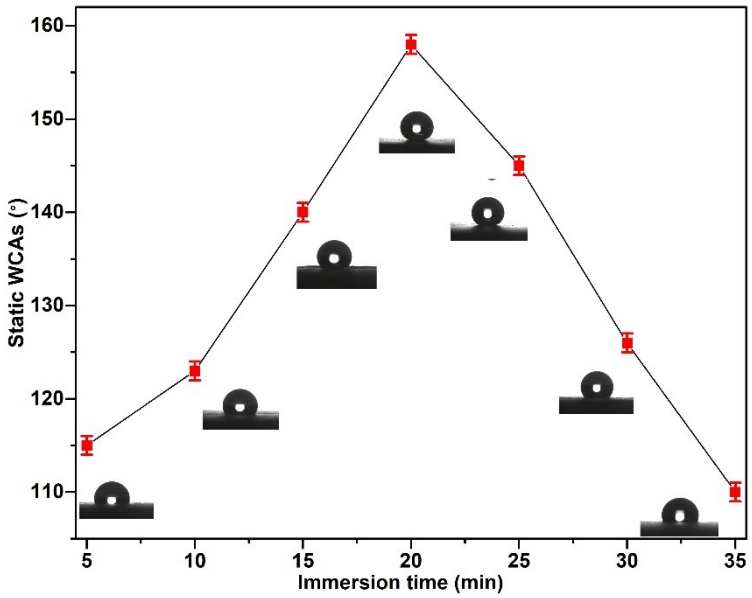

Fig. S4. WCAs of the as-prepared surfaces for 7 min in 2M HNO_3 solution while immersed in 5.5 mmol·L^{-1} $AgNO_3$ solution for 20 min, followed by annealing at 155 ºC for 1h along with different immersion times.

Our sharp observation for the immersion time is under 15 minutes, and the sizes of the dendritic structures that appeared in Fig. 3(c-f). Through the rise of time for immersion, the structures expanded progressively as the dependable dimensions appeared.

1.3. Annealing Temperature

Fig. S5 represents the static WCAs relation with annealing time and annealing temperature separately. After immersion, the copper alloy sheets were vertically dipped in a 5.5 mmol aqueous solution of silver nitrate for up to 20 minutes. After that, the substrate surface is thermally annealed in an electric oven at different temperatures (125, 135, 145, 155, 165, 175, and 185 °C), separately for 1 hour as seen in Fig. S3.

Moreover, the WCA obtained up to 146±1° except for the annealing temperature of 160 °C(Velayi and Norouzbeigi, 2018).

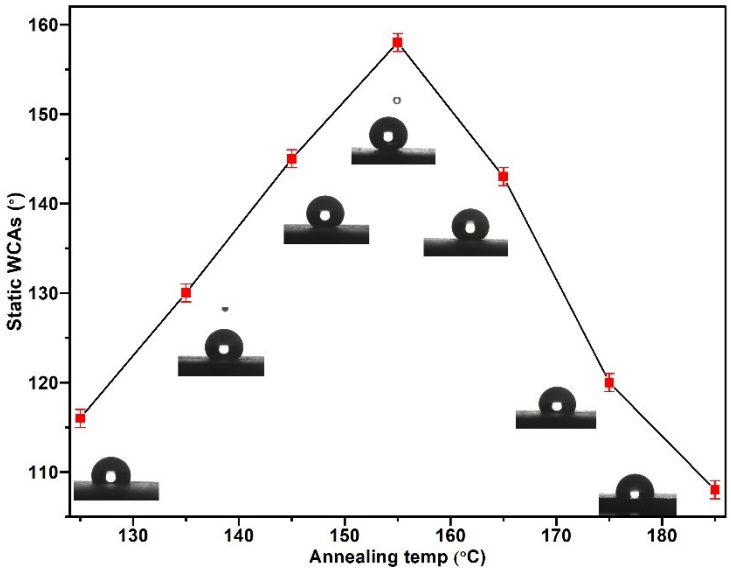

Fig. S5. WCAs of the as-prepared surfaces for 6 min in 2M HNO_3 solution while immersed in 5.5 mmol·L^{-1} $AgNO_3$ solution for 20 min, followed by annealing at 155 ºC for 1 h along with different annealing temperatures.

Subsequently, more mass-like structures showed up on the surfaces until the point when the surface was entirely secured with this new structure. Just with a reasonable immersion time, it fabricates the superhydrophobic surface. The experiment was repeated several times, especially for annealing temperature, and a perfect Ag-NPs @SHS was obtained only at 155°C.

1.4. Annealing Time

The annealing is a vital parameter to impart the superhydrophobicity on substrates (Zhao et al., 2022). The immersed copper alloy sheets were annealed at 155°C for different times (30, 40, 50, 60, 70, 80, and 90) minutes, individually shown in Fig. S6. The superhydrophobic surface with WCA greater than 140±1°and the SA above 12± 2° is determined after annealing the substrate at 155°C for 45 minutes. A perfect SHS (representing the WCA of 158±1° and SA of less than 2°) was fabricated when the annealing time and thermal annealing temperature were 60 minutes and 155°C. The thermal annealing time primarily affects the surface wettability. When the time was between 45 to 75 minutes, all results were measured, and the annealing temperature was assumed a vital tool for wettability. Thus, the annealing temperature (155°C) and annealing time (60 minutes) is the optimum condition.

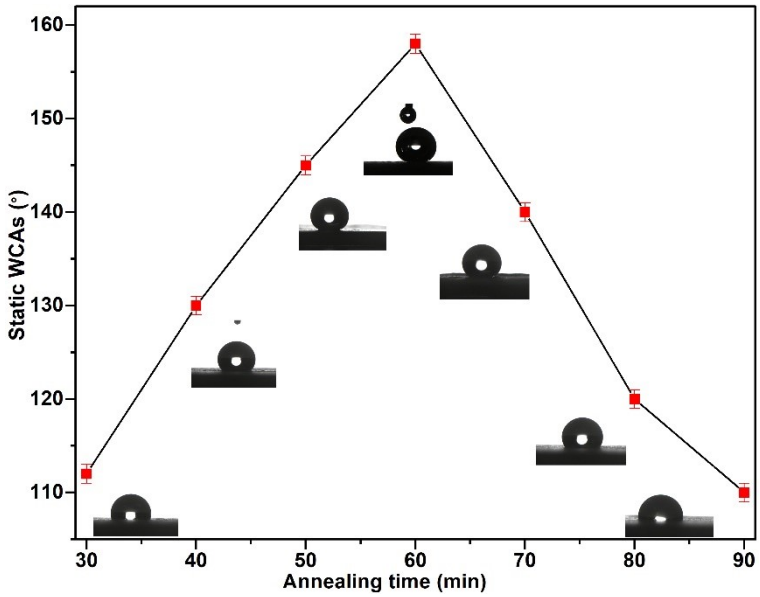

Fig. S6. WCAs of the as-prepared surfaces for 7 min in 2M HNO_3 solution while immersed in 5.5 mmol·L^{-1} $AgNO_3$ solution for 20 min, followed by annealing at 155ºC for 1 h along with different annealing times.

It was observed that at below and above thermal annealing temperature of 155°C the growth of beads-like spherical shapes of the Ag nanoparticles and their attachment on the copper substrate surfaces occurs, and even the surface morphologies are also affected by changing the time interval from 60 minutes. Sritharan et al, reported that Ag–Cu intermetallic is willing towards oxidation when thermally annealed Ag-Cu is kept in the open air, most likely showing a designing perspective, and both the annealing temperature and time impact: on the morphology, surface wettability, stability, robustness, and durability of the SHS(Xu et al., 2011). In our investigation, the ideal temperature of annealing and time is concluded. Just the perfect conditions directed that develop the ideal superhydrophobic surface.

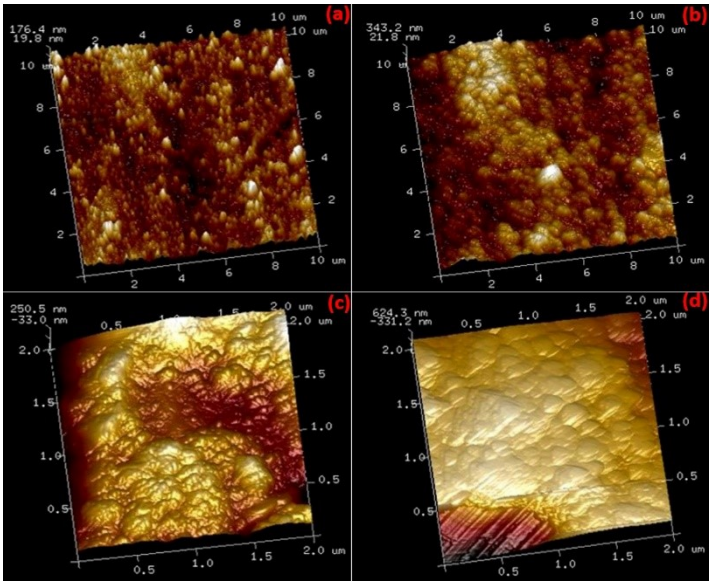

Fig. S7. 3D-images of surface morphology of samples captured by AFM: sample (W) is a non-coated copper alloy (a), sample (X) is the chemically etched sheet of copper alloy (b), sample (Y) is a sheet of copper alloy on which Ag-NPs were coated (c), and the sample (Z) was obtained after the thermal annealing of Ag-NPs coated copper alloy (d).

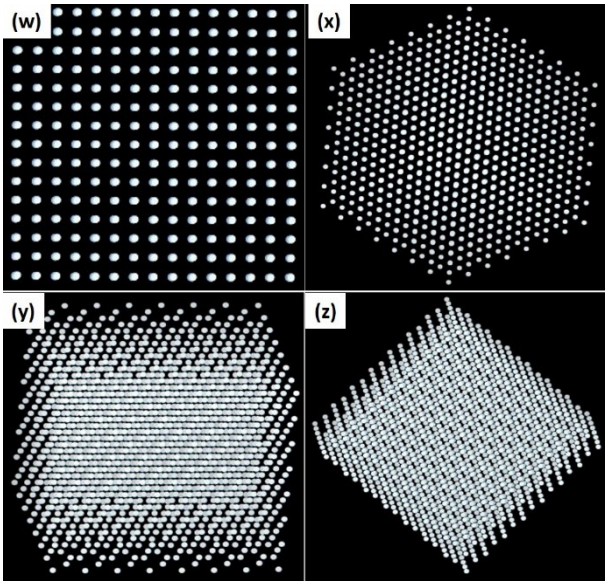

Fig. S8. Images of distribution of Ag-NPs. The 1D and 2D pattern of distribution of Ag-NPs (w and x), while the different views of the 3D texture of silver nanoparticles followed by annealing at 155 ºC for 1 h of annealing times.

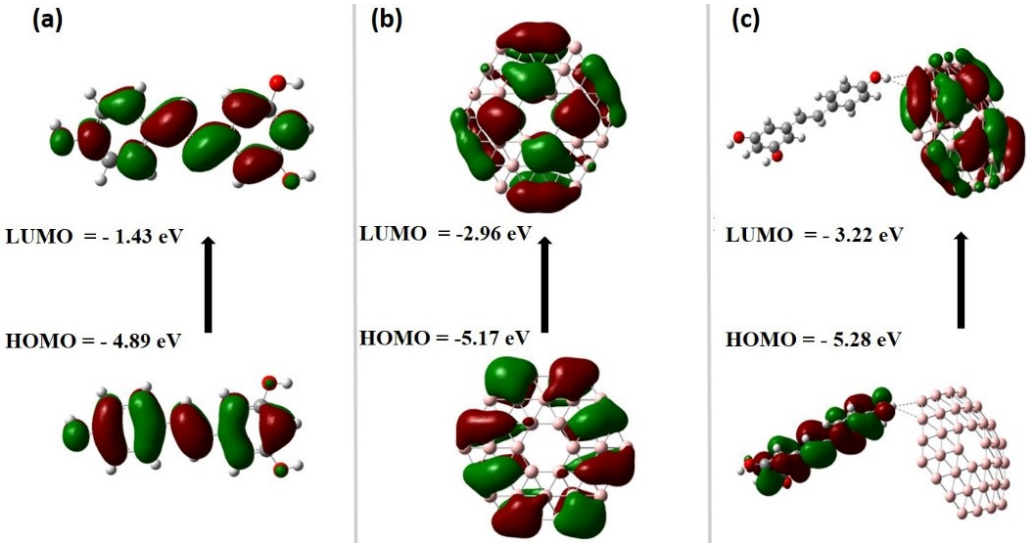

Fig. S9. The HOMO and LUMO of three molecular systems. (a) Ag-NPs, (b) Ag-NPs + SA and (c) Ag-NPs + SA @copper. LUMO is a universally known acronym for lowest unoccupied molecular orbital, whereas, HOMO is for highest occupied molecular orbital, in molecular orbital theory. The HOMO and LUMO energy levels of these molecular systems were likely investigated or compared, potentially through DFT calculation.

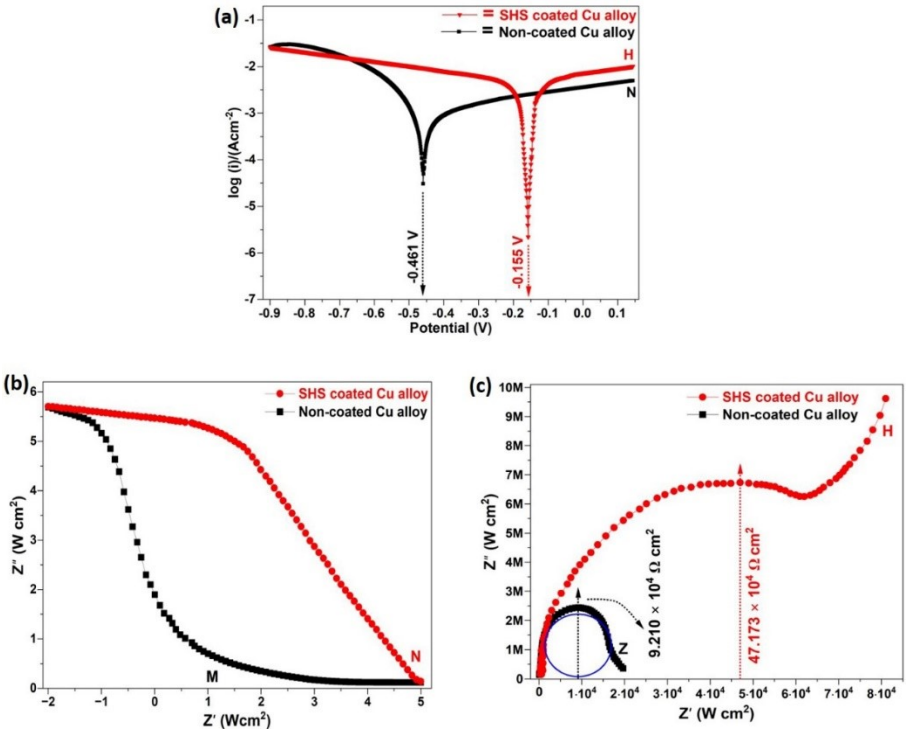

Fig. S10. EIS analysis of samples: Potentiodynamic polarization curves of non-coated and the Ag@SHS coated copper alloy. Bode modulus plots of bare copper alloy (curve M), and the (curve N) for Ag-NPs +SA@SHS of copper alloy, and the (c) indicated the curve (M) for non-treated copper alloy while curve (H) for Ag-NPs@SHS attained by Nyquist test.

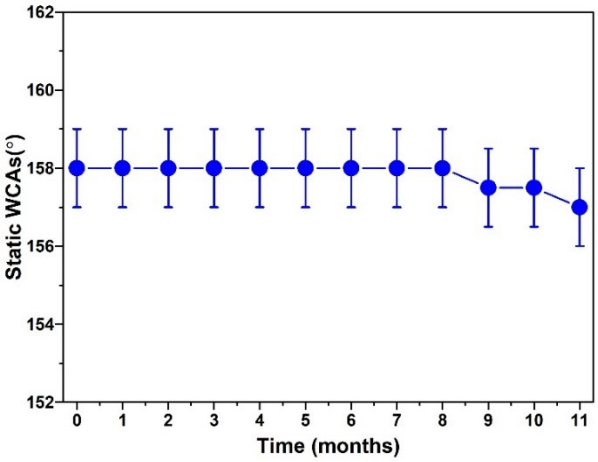

Fig. S11. Environmental stability of the coated sheet of copper alloy by Ag-NPs @SA.

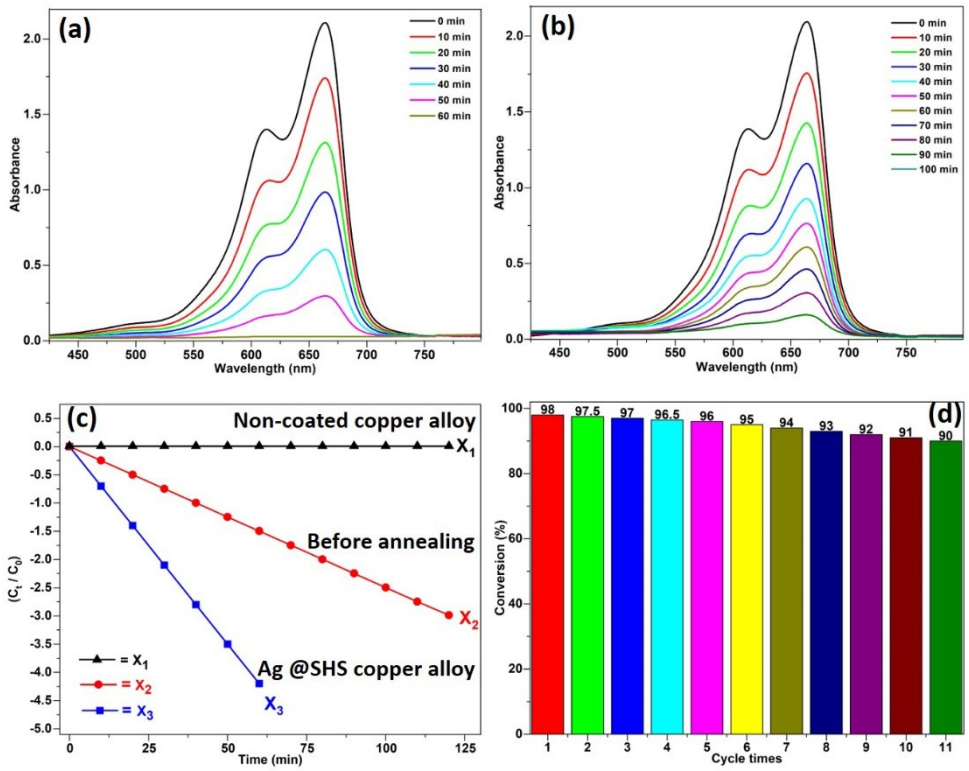

Fig. S12. U.V–Visible spectra of MB: MB in the presence of X_3 and reaction color change, (a). U.V–Visible spectra of MB in the presence of X_2, (b). The plots of ln (C_t/C_0) versus degradation time in the presence of X_3, X_2, and X_1 and photodegradation of MB versus the catalyst cycles for X_3 (d).

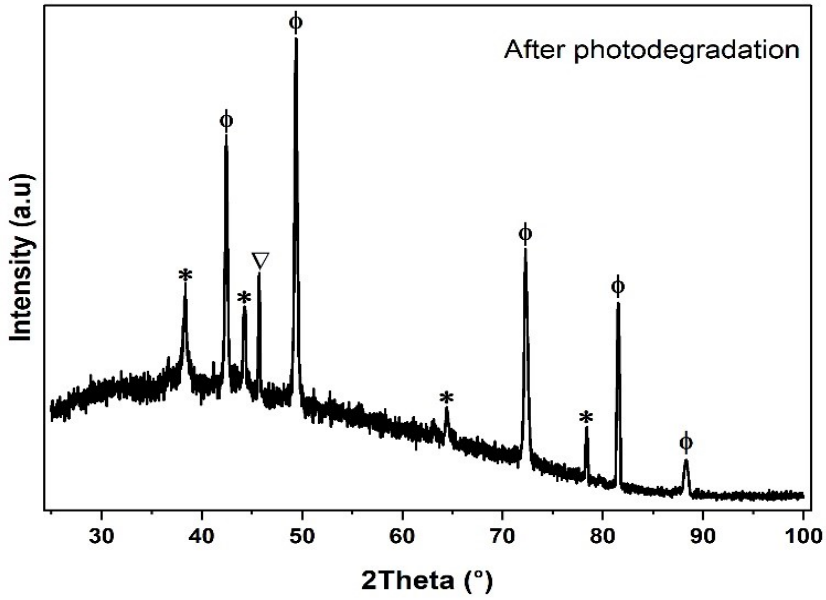

Fig. S13. Observation of the surface after photodegradation: (XRD) surface structure of Ag-NPs @SHS coated copper alloy.

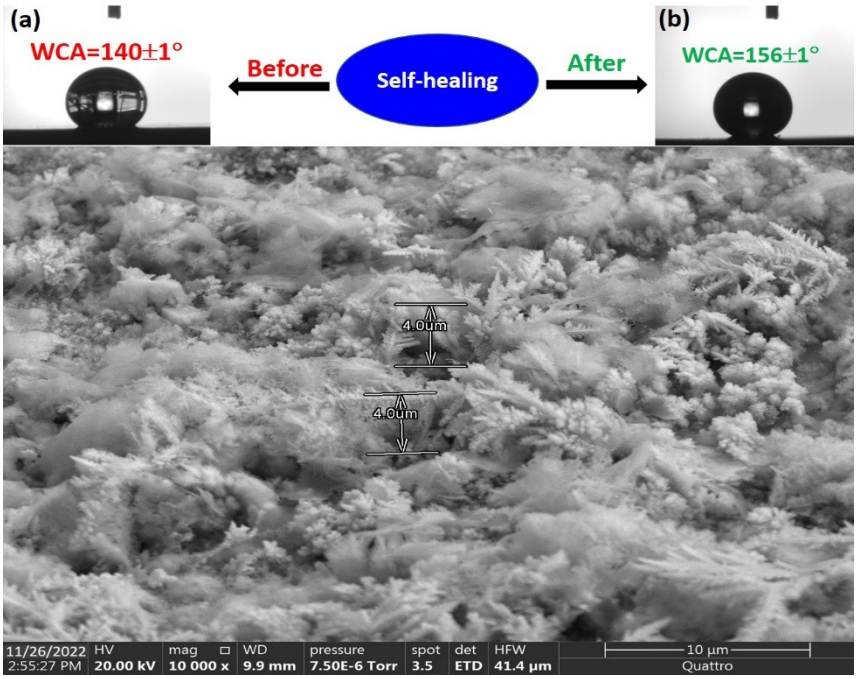

Fig. S14. Observation of the surface after photocatalysis: (XRD) surface structure of coated aluminum substrate (a), SEM image after several cycles of continuous degradation, and inset WCA of 140±1° before the self-healing (a) and after the self-healing along with WCA of 156±1°(b).

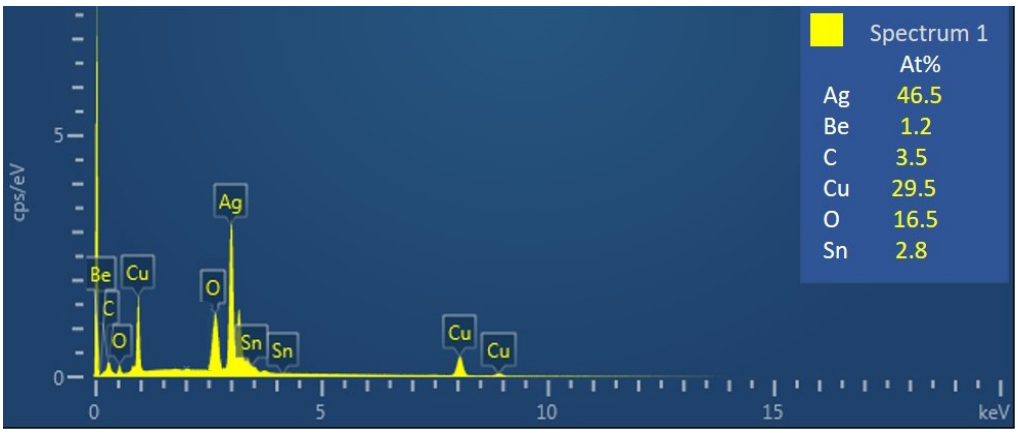

Fig. S15. Observation of the surface after degradation: Surface morphology of the superhydrophobic surface composed of Ag-NPs, fabricated on the copper alloy after photodegradation of the dyes.

Reference

Song, J., Xu, W., Liu, X., Lu, Y., Wei, Z., Wu, L., 2012. Ultrafast fabrication of rough structures required by superhydrophobic surfaces on Al substrates using an immersion method. Chemical Engineering Journal 211, 143-152.
Velayi, E., Norouzbeigi, R., 2018. Annealing temperature dependent reversible wettability switching of micro/nano structured ZnO superhydrophobic surfaces. Applied Surface Science 441, 156-164.
Wang, Y., Liu, X., Zhang, H., Zhou, Z., 2015. Superhydrophobic surfaces created by a one-step solution-immersion process and their drag-reduction effect on water. Rsc Advances 5, 18909-18914.
Xu, H., Liu, C., Silberschmidt, V.V., Pramana, S.S., White, T.J., Chen, Z., Acoff, V.L., 2011. New mechanisms of void growth in Au–Al wire bonds: Volumetric shrinkage and intermetallic oxidation. Scripta Materialia 65, 642-645.
Zhao, S., Du, H., Ma, Z., Xiao, G., Liu, J., Jiang, Y., Hu, S., Zhao, H., Wen, C., Ren, L., 2022. Efficient fabrication of ternary coupling biomimetic superhydrophobic surfaces with superior performance of anti-wetting and self-cleaning by a simple two-step method. Materials & Design 223, 111145.